

UNLIMITED

Communications Research Centre

SITE AND SYSTEM PHASE ERROR IN THE CRC HF SAMPLING ARRAY

by

L.E. Montbriand

COMMUNICATIONS CANADA
CRC

APR 13 1982

LIBRARY — BIBLIOTHÈQUE

This work was sponsored by the Department of National Defence, Research and Development Branch
under Project No. 33G01,

IC

DEPARTMENT OF COMMUNICATIONS
MINISTÈRE DES COMMUNICATIONS

CRC TECHNICAL NOTE NO. 710

CANADA

OTTAWA, OCTOBER 1981

LKC
TK
5102.5
.R48e
#710
c.2

COMMUNICATIONS RESEARCH CENTRE

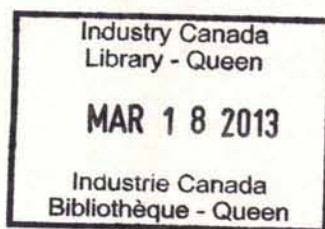
DEPARTMENT OF COMMUNICATIONS
CANADA

SITE AND SYSTEM PHASE ERROR IN THE CRC HF SAMPLING ARRAY

by

L.E. Montbriand

(Radar and Communications Technology Branch)



CRC TECHNICAL NOTE NO. 710

October 1981

OTTAWA

This work was sponsored by the Department of National Defence, Research and Development Branch under Project No. 33G01.

CAUTION

The use of this information is permitted subject to recognition of
proprietary and patent rights.

ADA 4504065
AL 5365730

TK
5102.5
R480
#910
c. b

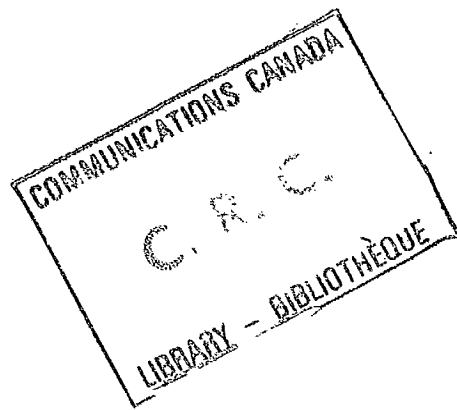


TABLE OF CONTENTS

ABSTRACT	1
1. INTRODUCTION	1
2. EXPERIMENTAL TECHNIQUE	2
3. DATA REDUCTION	6
4. SOURCES OF ERRORS	7
5. RESULTS	7
5.1 Empirical Determination of Residual Phase Errors (RPE)	7
5.2 Variation of Residual Phase Errors for a Small Change in Azimuth	8
5.3 Variation of Residual Phase Errors With Frequency and Time	8
5.4 Effects of Residual Phase Errors on Wavefront Nonlinearity	10
5.5 Effect of Residual Phase Errors on Bearing Measurements For Different Aperture Sizes	10
5.6 Variation of Measured Azimuth With Aperture Size	14
6. CONCLUSION	15
7. ACKNOWLEDGEMENTS	16
8. REFERENCES	16

SITE AND SYSTEM PHASE ERROR IN THE CRC HF SAMPLING ARRAY

by

L.E. Montbriand

ABSTRACT

The CRC HF sampling array is comprised of a number of parallel channels. Each channel consists of an antenna element, a coaxial cable, and a radio receiver. The receiver outputs are digitized for subsequent processing. The relative phase shift imposed on a signal in passing through each channel can be estimated using various calibration procedures. There still remains, however, in each receiving channel a residual error in the phase that seems to vary from receiver-to-receiver across the aperture of the array in a systematic way. The RMS value of this error is about 3-4° when averaged over a large number of receiving channels, but peak errors can be as large as 10 to 15°. For frequencies near 6 MHz this system/site error can lead to a bearing error of up to 0.2°, when a subset of elements with an 84 m aperture (out of the 1943 m aperture) is used for the bearing determinations. Improving bearings by this magnitude would be important only when the wavefronts are very linear as is the case for the E mode. A bearing error of 0.2° is normally masked by much larger bearing variations due to ionospheric propagation effects.

1. INTRODUCTION

The H.F. Sampling Array (Rice and Winacott¹) operated by the Communications Research Centre, Ottawa, includes a number of antennas in two arrays at right angles with each antenna connected to its own receiver. During operations, the in-phase and quadrature components of each receiver output signal are digitized and recorded. The components are subsequently analyzed for amplitude and phase. From the set of phases it is possible to find the azimuth and elevation of an incoming signal. A previous report (Burke²) has described the procedure for calibrating the gain and phase characteristics

of the receiver portion of each channel. Other checks which are made routinely include verification that the antenna elements and cable system are functioning as intended. After such care there still remain phase errors which are random (due to noise, etc.) as well as a component which is systematic in nature. This component, although not large, can be estimated in some cases, when the RMS of phase errors across the aperture is small, e.g. for signals propagated via single ionospheric modes. The purpose of this note is to describe a technique for estimating these errors and to indicate the effect that inclusion of these error corrections would have on the various direction finding parameters as measured by the sampling array.

2. EXPERIMENTAL TECHNIQUE

The experimental arrangement used for results reported herein is similar to that reported in Rice³ and Rice and Winacott¹. A swept frequency continuous wave (SFCW) signal was transmitted from Sept Iles, Quebec (50°12'N, 66°09'W) and received at Ottawa (45°14'N, 75°51'W). An experiment was carried out between 20 June and 23 June 1977 using a 50 KHz swept bandwidth and frequencies ranging from 5.2 to 7.7 MHz.

For the results reported here, the sampling array had a total aperture of 1943 m in the long arm. This was accomplished by adding 4 additional antenna elements along the original 1181 m arm in the northwest direction at the locations 1332, 1561, 1741 and 1943 m.

Data processing was carried out in such a way as to independently study 9 aperture sizes on the long arm (plus an alternative one for 1181 m) and 3 aperture sizes on the short arm. Details of these 13 apertures are presented in Table 1 and their position in the array arms can be identified by the receiver numbers along the lower scale in Figures 1 and 3.

TABLE 1
List of Apertures

Aperture (Meters)	Long Arm	Last RCVR
	First RCVR	
84	23	28
145	21	30
267	17	34
419	15	36
572	13	38
800	9	42
1181A	5	46
1181B	1	16
1562	3	46
1943	1	46
	Short Arm	
84	52	57
145	50	59
236	47	62

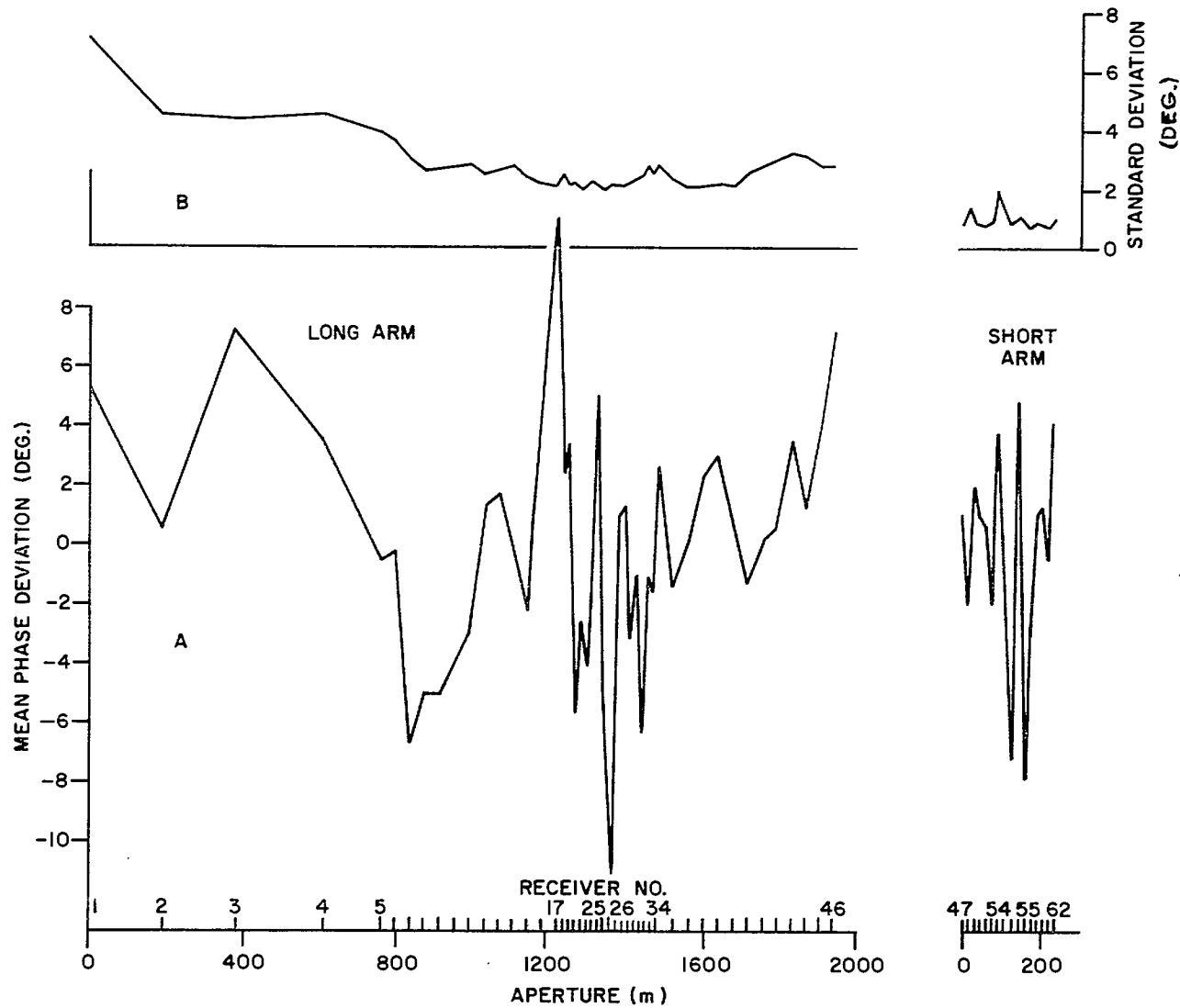


Figure 1. (a) Mean Phase deviations (residual phase errors) of receiver phases for long and short arms of the HF sampling array vs antenna position (and receiver number) for day 171 12:23-13:54 EST at 6.90 MHz for low angle E mode, (b) standard deviation of mean phase deviations of (a). The Long arm results are for 29 sets of phase deviations and the short arm results for 55 sets.

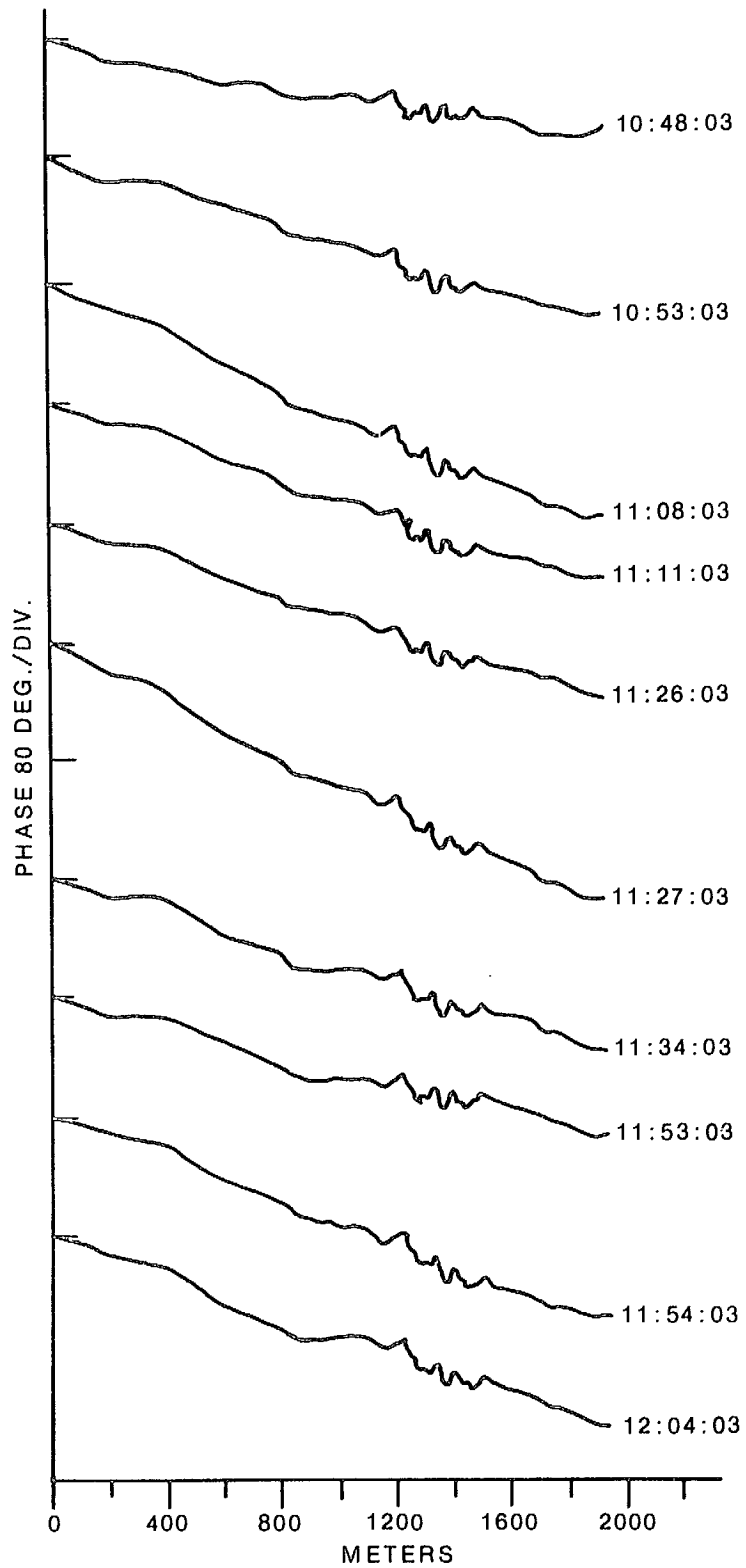


Figure 2. Phase fronts along the long arm for selected low angle E mode transmissions over the Sept Iles to Ottawa path on day 171, 1977 at 6.95 MHz.

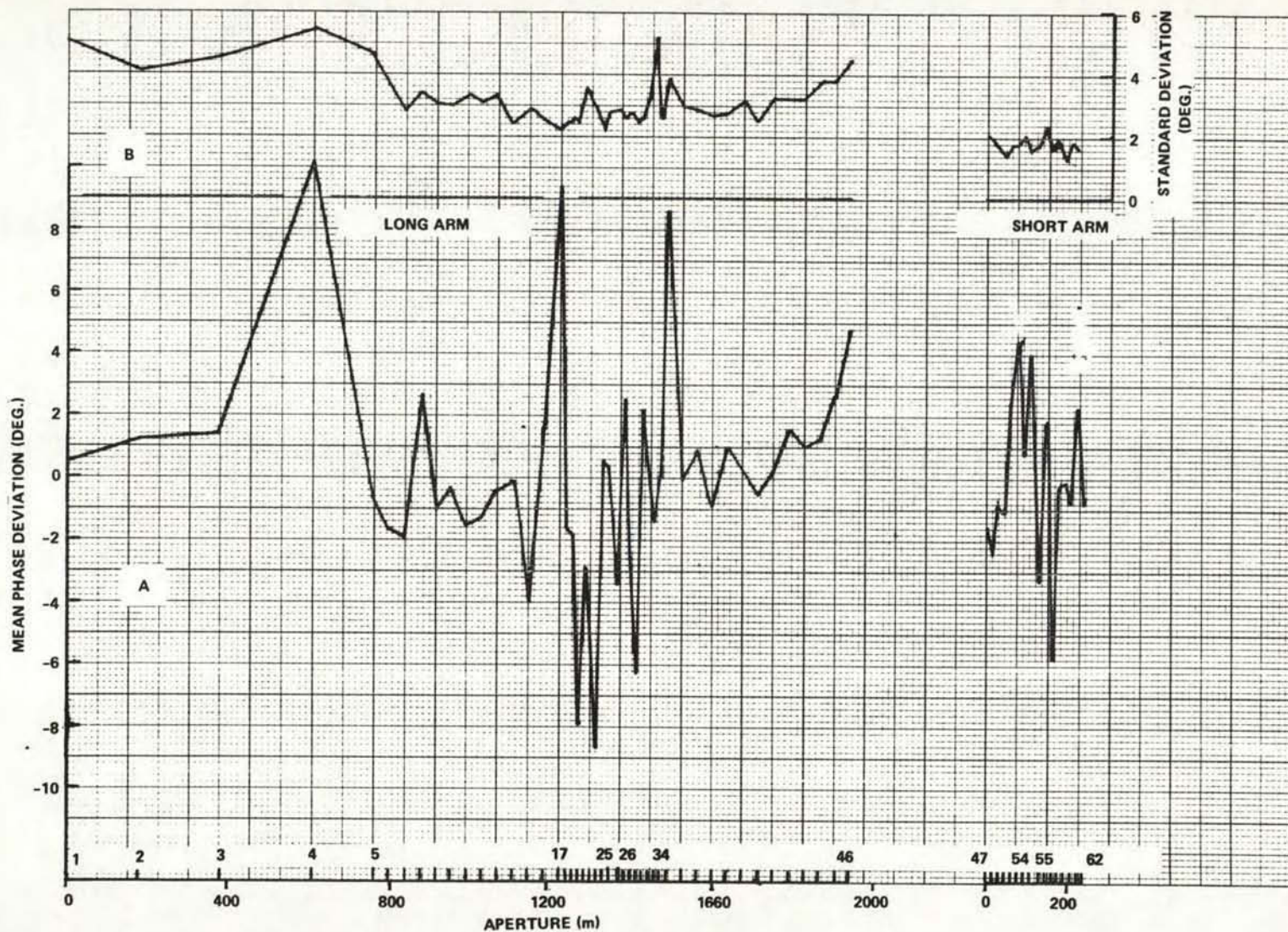


Figure 3. (a) Mean Phase deviations (residual phase errors) of receiver phases for long and short arms of the HF sampling array vs antenna position (and receiver number) for day 173 08:32-17:49 EST at approximately 6.9 MHz for low angle F2(o) mode, (b) standard deviation of mean phase deviations of (a). The long arm results are for 44 sets of phase deviations and the short arm for 116 sets.

3. DATA REDUCTION

The data collection and processing techniques during the test were similar to those used by Rice⁴ but incorporated the calibration procedure as outlined by Burke². The recorded data were processed in two stages. In the first stage, receiver phase corrections obtained from the calibration procedure were incorporated, as well as phase corrections for differences in cable lengths (Rice and Winacott¹). During this stage of analysis, data were processed for range. The resulting output magnetic tape thus contained data presented in time-delay (range) vs receiver number coordinates with each data point being a complex representation of signal amplitude and phase. In the second stage of processing, calculations were carried out on ranges with significant signal strength to determine phase slope, cone angle and wavefront quality for each arm of the array. A linear fit of the phases over the aperture was used to obtain the phase slope. A measure of wavefront quality was determined by calculating the root mean square (RMS) of phase deviations from the straight line fit to the phase measurements over the receiving aperture. These phase deviations for each receiver make up what are herein referred to as a "set of phase deviations" and are for a 2 s sample of data taken once a minute. Since the antenna spacings were not uniform, see Figures 1 and 3, which show that the antennas are more closely spaced near the centre of the array, the individual phase deviations were weighted. This was accomplished by multiplying the individual phase values by the mean distance to its adjacent antennas divided by the mean distance between antennas in the array, which is the weighting that would be applied in analyzing data for an array with uniform spacing. Herein the term SDPH refers to the RMS values of such weighted phase deviations.

The cone angle (the angle between the axis of the arm of the array and the normal to the wavefront) is evaluated as $360/2\pi \text{ arc sin } (ac/(360f))$ where a the slope of the wavefront normal (in degrees/m), is derived from the least squares straight line fit. In the equation, c is the velocity of light and f the received frequency. The cone angle accuracy is dependent upon the accuracy of the slope a .

The orientation of the array is such that the long arm is almost perpendicular to the Sept Iles to Ottawa path. As a result, the azimuth of the arriving transmissions is approximately the same as the cone angle measured by the long arm. Hence in this note the cone angles of the long arm are referred to as azimuths or azimuthal cone angles and cone angles of the short arm as elevations or elevation cone angles. Numerically the cone angle and its corresponding azimuth or elevation differ significantly, e.g., in Figure 8 an azimuth of 49.2° corresponds to an azimuthal cone angle of 89.58° and an elevation of 10.0° and an elevation cone angle of 170.2° .

Although the minimum inter-element spacing used in the experiment was 15.24 m, a 22.86 m spacing at the centre of the array, when used in conjunction with neighbouring elements in a phase resolving algorithm provided a single effective spacing of 7.62 m corresponding to one-half wavelength at 19.7 MHz. Frequencies used were always below this value. It was assumed that 2π ambiguities in the phase measurements from the more widely-spaced elements in the long array were properly resolved by extrapolating the phase slope obtained from the closely-spaced elements.

Separation of modes on the basis of differential time delay was accomplished at the first stage of processing. Identification of the modes was then made by comparison of the data with oblique ionograms which were produced at 20 minute intervals during the course of the experiment. In some cases identification was aided by the azimuth and elevation information available from subsequent processing.

4. SOURCES OF ERRORS

Before discussing the results to be presented in this note, let us consider sources of possible error. The main source of error, resulting in non-linearity of the wavefront is ionospheric in origin and results from the simultaneous presence of two or more ray paths, with each ray having its own incident elevation and azimuth angles. Here we are concerned with a study of data when phase deviations due to propagation were smallest, that is, we are attempting to determine the residual phase errors due to the site and system. Site errors could arise because of secondary reflections from fences, power lines, etc. System errors could be due to the non-symmetric ground-screen beneath the antenna arrays, to mutual impedance between elements, particularly at array intersections and at locations where the element spacing changes, etc. The purpose of this study is to estimate the magnitude of these site/system errors and to deduce the effect they have on bearing accuracies.

5. RESULTS

Examples of phase fronts exhibiting systematic waves are shown in Figure 2. On it are plotted ten selected phase fronts for the low angle E mode for June 20, 1977 (Day 171) for the Sept Iles to Ottawa path. The most obvious characteristic of these phase fronts is the repeatability of the phase deviations observed, particularly in the 1100-1500 metre aperture distance where the antennas are more closely spaced. In this part of the trace, one can see that the variation has a pattern that does not change with time, that is, the deviation observed must be due to systematic errors due to the site and system. These errors due to site and system can be evaluated as residual phase errors (RPE).

5.1 EMPIRICAL DETERMINATION OF RESIDUAL PHASE ERRORS (RPE)

In order to determine the RPE for the entire array, various sets of phase deviations for a selected mode were compiled for which the mean phase deviations over the largest aperture of each arm were each less than 6° . These sets of phase deviations were then processed to determine for each receiver the average of the phase deviations and their standard deviation. In Figure 1, which presents results for the low angle E mode at 6.9 MHz, between 12:23-13:54 EST, the lower graphs show the mean of the phase deviations as a function of antenna position for both the long and the short arm of the crossed array. The results on the left are for the 1943 m aperture on the long arm (azimuthal cone angle) while those on the right are for the

236 m aperture on the short arm (elevation cone angle). For the former the SDPH is $<6^\circ$ and for the latter $<4^\circ$. As can be seen for the long arm, the mean of these phase deviations in the receiver was as large as $\pm 10^\circ$, and on the short arm as large as $\pm 6^\circ$. These errors are considerably larger than the changes in phase that a receiver may undergo between calibrations which is usually less than $\pm 2^\circ$ but may be as high as $\pm 5^\circ$ for a few receivers.

Figure 3 presents similar results for the low angle F2(o) mode at approximately 6.9 MHz between 08:32-17:49 EST. A visual comparison of Figures 1 and 3 reveals an overall similarity, but there are differences in detail between them.

5.2 VARIATION OF RESIDUAL PHASE ERRORS FOR A SMALL CHANGE IN AZIMUTH

In an attempt to obtain more accurate RPE, such errors were determined for azimuth differences of near one-half a degree. Data for the low angle E mode along the great circle propagation direction on Day 171 for frequencies 6.97 to 7.10 MHz was used. There were 167 cases with SDPH $< 10^\circ$, and azimuths ranged from 48.8 to 49.6° with a median of 49.15° . Residual phase errors were determined for the 14 cases with azimuth $< 49.0^\circ$ and 24 cases with azimuth $> 49.3^\circ$. The residual phase errors for both azimuthal directions were essentially identical indicating that for the low angle E mode transmission from a known transmitter such as Sept Iles, one set of residual phase errors for the range of frequencies indicated, would be satisfactory for the narrow range of azimuths that would normally occur. On a similar test for the F1 low angle mode, for which the azimuthal spread is much greater than for the E mode, this was not true. The results seemed to indicate that the residual phase errors could change noticeably for an azimuth change of a few degrees and/or an elevation change of 5° . However, if the SDPH over the long arm approaches 10° for azimuth and elevation spreads of this magnitude, as is the more common case, there is little to be gained in determining RPE as the error component from ionospheric propagation is the dominant one. A more careful study of this problem is needed to verify this conclusion.

5.3 VARIATION OF RESIDUAL PHASE ERRORS WITH FREQUENCY AND TIME

The variation of the RPE with frequency is illustrated in Figure 4 for 7 of the 62 receivers. Note that the results are broken down into three widely separated ranges of frequency. As can be seen, the RPE are dependent on frequency and change measurably for frequency changes as small as 0.25 MHz.

It was also found that RPE obtained for one day could not necessarily be used on a date several days removed. The errors which contribute to the uncertainty in the receiver phases can be significantly different at different times. On one test, RPE for Day 171 were used on Day 173 with the result that, on the long arm, the median value of the SDPH for the 84 m aperture was reduced from 4.8° to 1.0° . However, the azimuthal cone angle for the 84 m aperture moved away from the great circle direction by 0.2° . On the other hand, when the RPE for the right day (173) was used, the azimuth moved toward the great circle direction by 0.1° . This 0.3° difference,

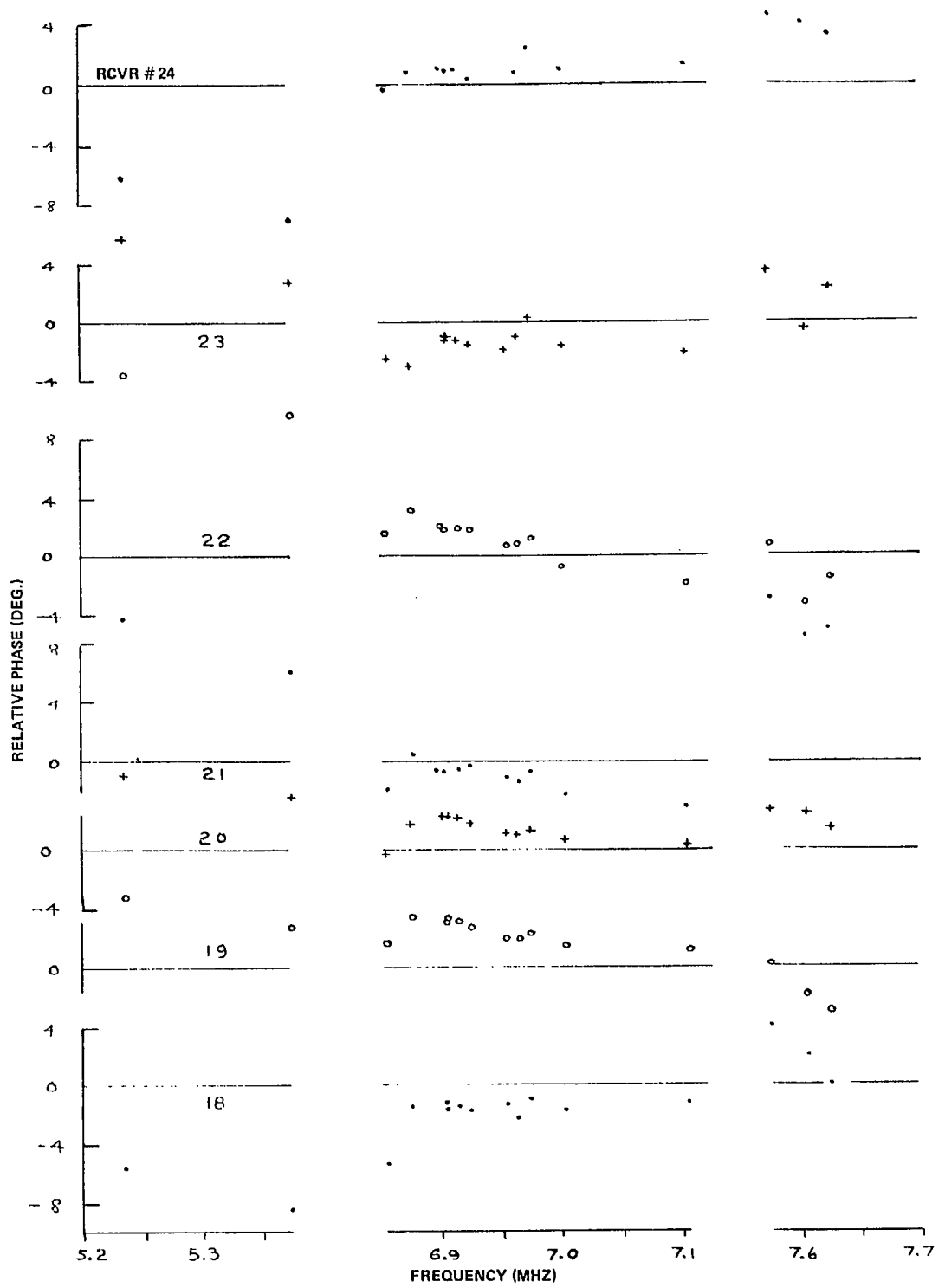


Figure 4. Variation of residual phase errors with frequency for the low angle E mode for receivers 18 to 24 (c.f. Figure 1 for position in array). The bars delineate the frequency intervals and help identify the variation with frequency.

although small was well in excess of the 0.06° standard deviation for the 84 m aperture (c.f. error bar in Figure 8A).

5.4 EFFECTS OF RESIDUAL PHASE ERRORS ON WAVEFRONT NONLINEARITY

For the 1943 m aperture of the above tests, less than 20% of the occurrences of the azimuthal cone angle for the low angle E mode had values of SDPH $> 20^\circ$. In Figure 5A, which illustrates for 5 selected apertures the probability that the SDPH exceeds the value plotted, 15.5% exceeded 20° for the 1943 m aperture. The removal of the RPE (Figure 5B) has the effect of reducing the values of the SDPH, an effect which can be appreciated by comparing the two diagrams in Figure 5. It can be seen more clearly in Figures 6 and 7 where the median value of the SDPH distributions is plotted as a function of aperture size for two different modes. On these figures, curve A represents results of processing without removing the RPE, and the curve B, results when the RPE are removed. Values of the SDPH are reduced to 2° from 5° , to 5° from 7° and to 10° from 11° for the 1943 aperture. For a value of the SDPH in excess of 15° , removal of these RPE has essentially negligible effect on the SDPH. The reason for this is that irregularities in the wavefront for such high values of SDPH are believed to be predominantly from multipath and/or multimode interactions. Curve C is obtained from Curves A and B where C is the square root of $(A^2 + B^2)$. Curve D is the equivalent of Curve C based on the weighted RMS of the phase deviations over the appropriate aperture.

The nature of the change in the value of SDPH from Curve A to B indicates an adding of variances. This indicates that the RPE are statistically independent of other errors.

5.5 EFFECT OF RESIDUAL PHASE ERRORS ON BEARING MEASUREMENTS FOR DIFFERENT APERTURE SIZES

A plot of the azimuthal and elevation cone angles as a function of aperture size is presented in Figure 8 for two of the test periods. The solid lines represent data without removal of the RPE, and the dashed lines, data with the RPE removed. Bars indicating the estimated error in mean cone angle (standard deviation of the mean cone angle \div square root of occurrences) are attached to the values for which RPE were removed. In addition, for the 84 m aperture of the short arm only, the standard deviation of the cone angle is shown by a dashed bar. As already mentioned, the cone angle of the long arm approximately represents the azimuth, and the cone angle of the short arm, elevation, and these scales are shown as the second ordinate scales in Figure 8. For the long arm the removal of the RPE changed the mean azimuthal cone angles (change from full line to the dashed line) for the worst case, the 267 m aperture, by as much as 0.2° , and this change was greater than the error in the mean azimuthal angle. For the short arm the change in the elevation cone angle resulting from the removal of the RPE was between 1° and 2° and far exceeded the error in the mean elevation cone angle for the 84 m aperture, and was as large as the standard deviation in the mean elevation cone angle.

As a means of establishing unambiguously that such changes in cone angle were systematic, (i.e., from system and site errors) three additional tests were run. On a test run on Day 171, 12:23-13:54 EST at 6.9 MHz on the low angle E mode, after removal of the RPE, the mean changes in cone angle on the long arm were $+0.07^\circ$, $+0.13^\circ$, $+0.03^\circ$ and 0.00° for the 84, 267, and 1181 and 1943 m apertures, and on the short arm $+2.1^\circ$ and 0.0° for the 84 and 236 m apertures. The standard deviation in the mean changes was $<0.01^\circ$, revealing that the mean changes in bearing was a result of a bias in the bearing artificially produced by the RPE. Note that the mean change in azimuth that can be expected over the full aperture is zero if the data used to obtain this mean is exactly the same as used to determine the RPE. If, on the other hand, the data used to obtain the mean includes additional cases, the change in the mean azimuth over the full aperture can be non-zero, e.g., Figure 8B.

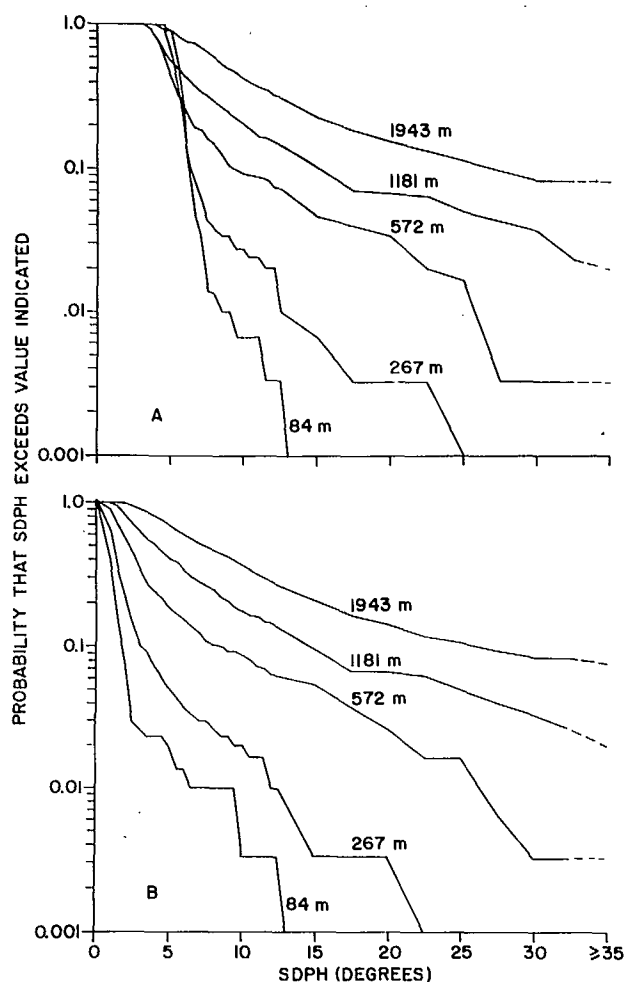


Figure 5. Probability that RMS phase deviation exceeds value indicated for case (A) without removal of residual phase errors and (B) with residual phase errors removed. E mode on day 171 09:05-15:14 EST at approximately 6.9 MHz.

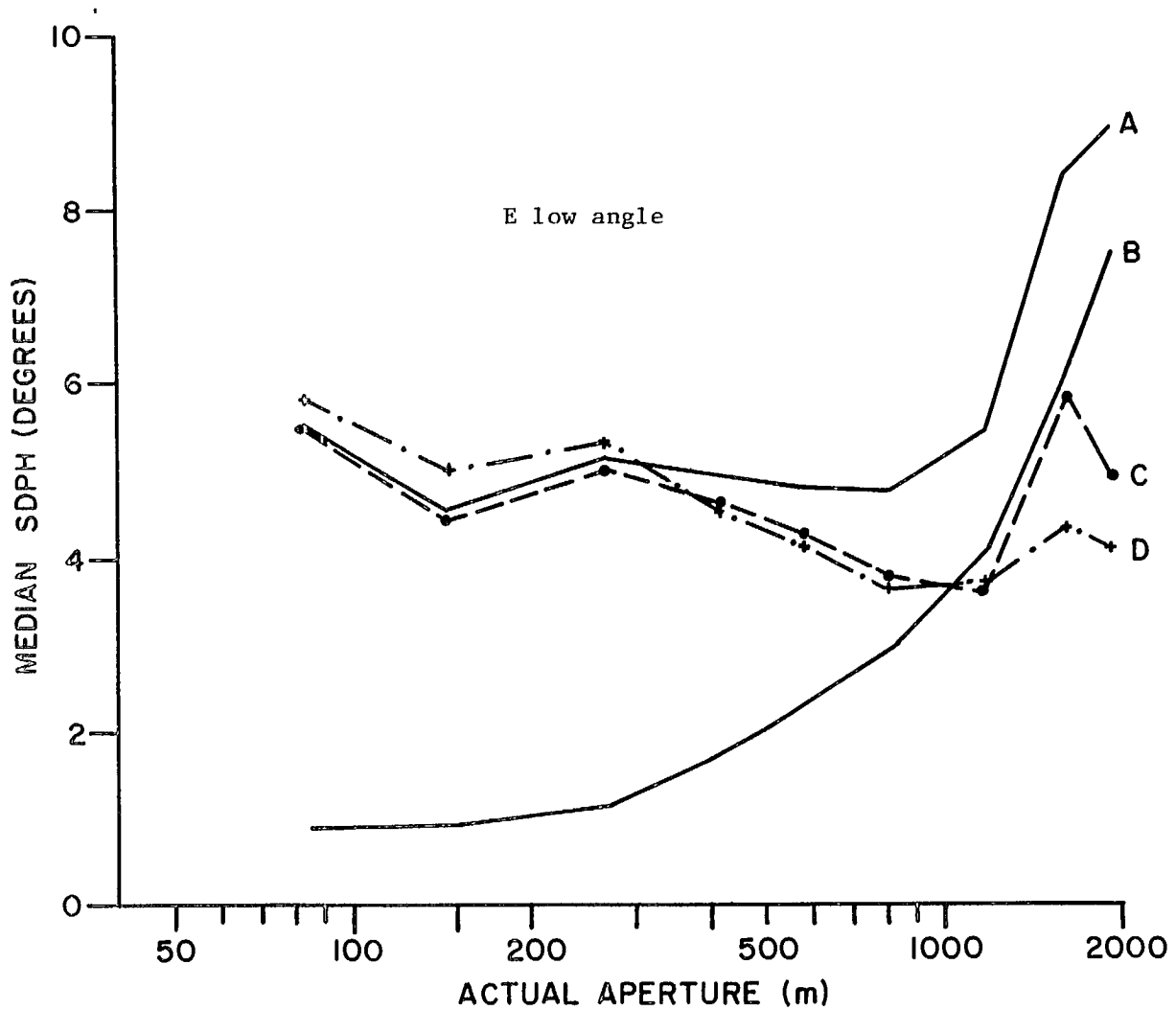


Figure 6. Estimated median SDPH vs aperture size for day 171 09:05–15:17 EST for the low angle E mode. Curve A – without removal of residual phase errors; Curve B – with residual phase errors removed; Curve C – power difference between curves A and B; Curve D – RMS of residual phase errors of applicable antennas in aperture.

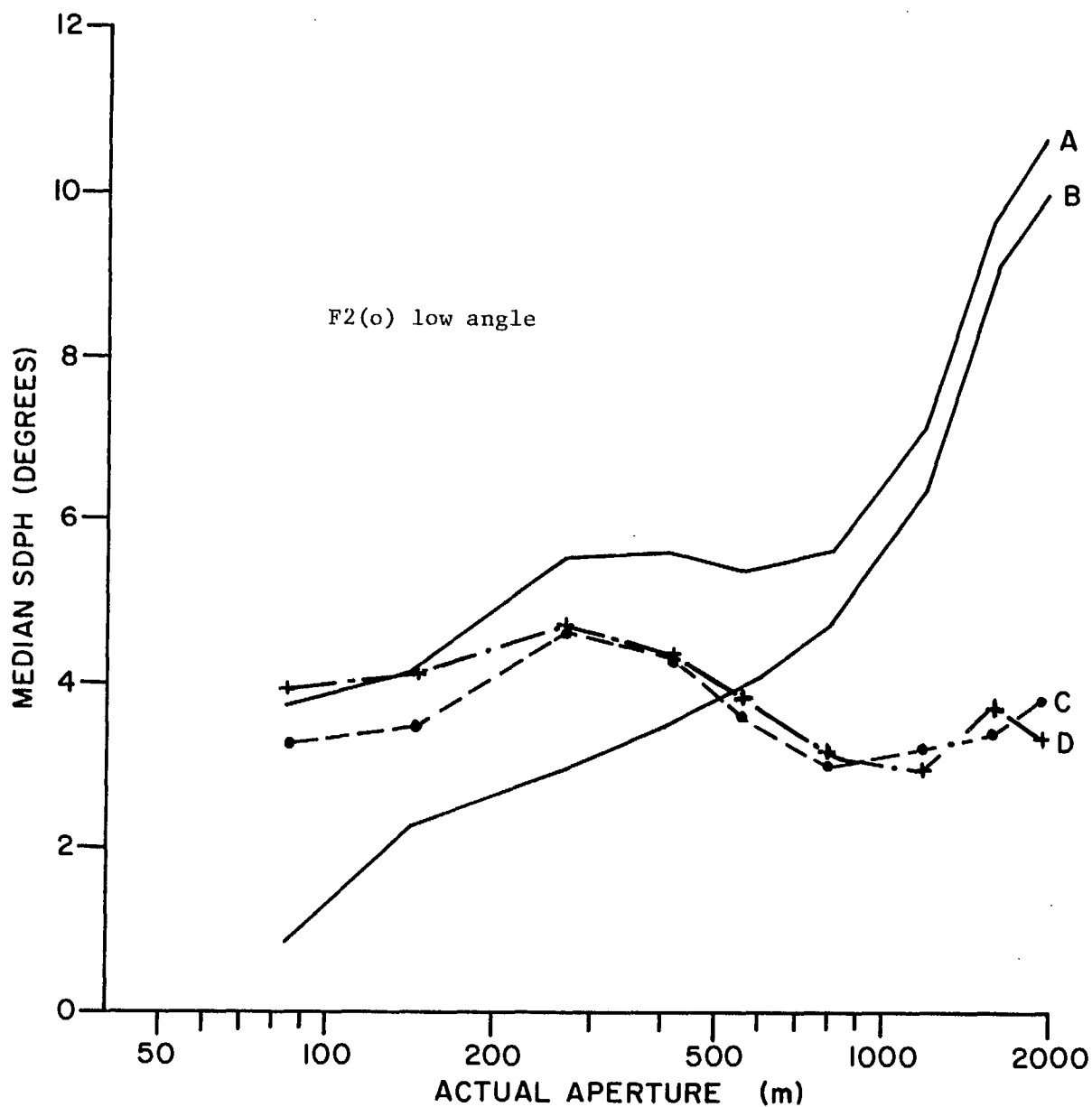


Figure 7. Variation of residual phase errors with frequency for the low angle F2(o) mode day 173 08:32-17:39 EST.

Curve A - without removal of residual phase errors; Curve B - with residual phase errors removed; Curve C - power difference between curves A and B; Curve D - RMS of residual phase errors of applicable antennas in aperture.

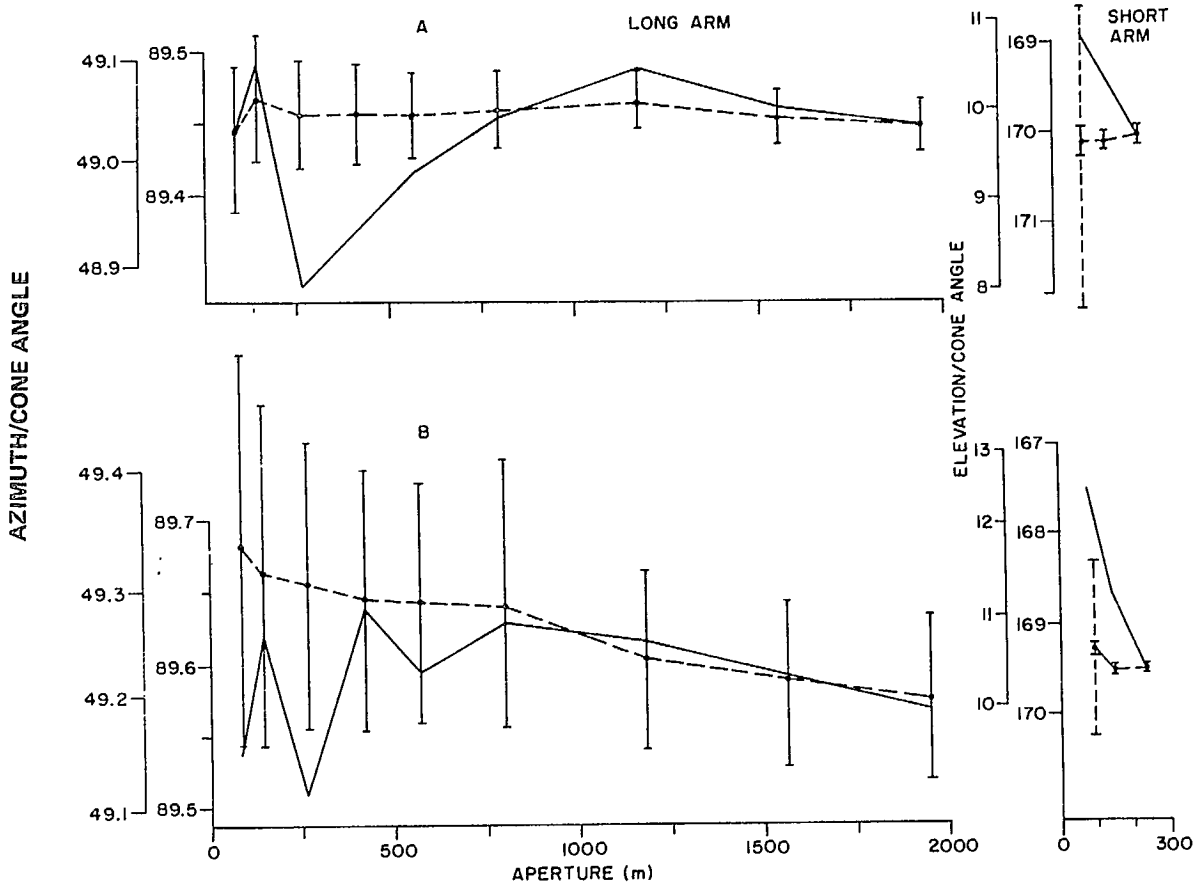


Figure 8. Mean cone angle vs aperture size for (A) day 171 09:15–15:14 EST and (B) day 172 11:00–12:23 EST for the low angle E mode. The cone angle of the long arm (89°) approximates the azimuth (49°) while that of the short arm (169°) approximates the elevation (11°). Dashed lines join values for which residual phase errors were removed, full lines join values for which residual phase errors were not removed. Solid bars represent estimated error of the mean and dashed bars, the standard deviation.

5.6 VARIATION OF MEASURED AZIMUTH WITH APERTURE SIZE

The dashed line in Figure 8B illustrates an example of the variation of measured azimuth with aperture size where the azimuth changes from $N49.35^\circ$ at 84 m to $N49.22^\circ$ at 1943 m. This change could be a result of the type of data reduction used. Such a change with aperture can be seen in results when multipath or multimode interference is present. Figure 9 is used to explain how such a behaviour shows up in the results. The upper diagrams indicate the bearings of two main incoming rays, the stronger directed vertically with the weaker to the right on the diagrams on the left, and to the left on the right diagrams. The lower diagrams illustrate the wavefront at the receiving array. The corrugation shown in the wavefront is due to the multipath interference. A theoretical treatment of the type of effect which produces such corrugations is given in Rook⁵. On the lower diagrams the average wavefront lies along the line CD which is drawn perpendicular to the direction of the stronger ray. This, the mean bearing, according to Gething⁶

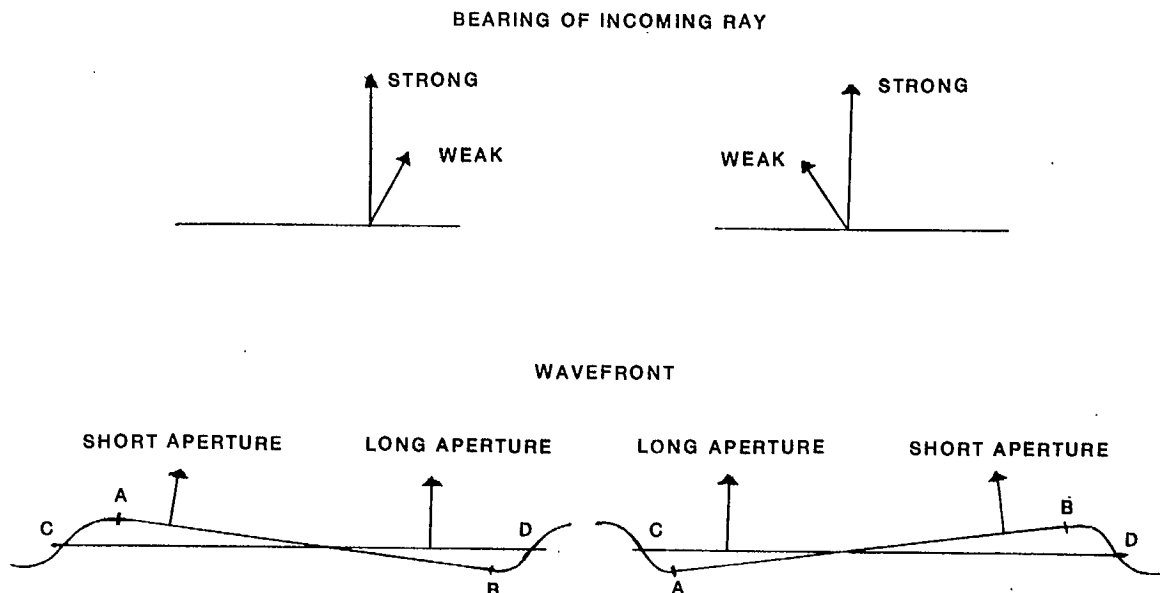


Figure 9. Illustration of wavefront produced by two signals, the strongest from the vertical direction. Lower diagrams illustrate wavefront. Most probable direction of wavefront measured is shown by arrow and labelled short for the 84 m aperture and long for the 1943 m aperture.

will be the same for all apertures if all phases are allowed for and will be the bearing of the strongest ray. In the type of data processing we carried out, most of the cases when a minor wavefront corrugation fell within the smallest apertures were rejected from further analysis because the wavefront was too non-linear, whereas many of the cases when a minor wavefront corrugation fell somewhere within the largest aperture were accepted. The result would be that the bearing for the short aperture was close to being perpendicular to the line AB rather than to the line CD. The observed change in apparent azimuth with aperture size could, at least in part, be attributed to this effect of the wavefront linearity test.

6. CONCLUSION

High frequency transmission tests were carried out in June 1977 on a 1943 m by 236 m crossed sampling array operated by the CRC. The RMS of residual phase errors (RPE) due to the system and the site is about 3 to 4° when averaged over a large number of receiving channels. Peak values in the RPE are about 10-15° for the worst channels. For frequencies near 6 MHz systematic site errors can lead to bearing errors up to 0.2° when a subset of the elements corresponding to apertures as small as 84 meters is used for bearing determinations. The possibility of making bearing error corrections by incorporating RPE is confined to those ionospheric modes for which the residual phase error component dominates over the ionospheric propagation component, such as is the case for the E mode. Removal of the RPE will not, however, remove errors in azimuth resulting from ionospheric tilts, e.g., in

Figure 8A the measured azimuth is 49.05° whereas the true azimuth of the transmission is 49.25° . The small improvement in the accuracy of the bearing produced by incorporating the RPE would render unimportant attempts to refine the technique for obtaining such residual errors.

7. ACKNOWLEDGEMENTS

The author thanks Drs. D.W. Rice and G. Atkinson for fruitful discussions and comments. This work was supported by the Department of National Defence of Canada.

8. REFERENCES

1. Rice, D.W. and E.L. Winacott, *A Sampling Array for the H.F. Direction-Finding Research*, CRC Report 1310, October 1977.
2. Burke, M.J., *Calibration of the CRC High-Frequency Direction Finding Receiver Systems at Ottawa*, CRC Tech Note 690, February 1978.
3. Rice, D.W., *Phase Characteristics of Ionosphericly Propagated Radio Waves*, Nature Physical Science, 244 #136, 86, 1973.
4. Rice, D.W., *High Resolution Measurements of Time Delay and Angle of Arrival Over a 911 km HF Path*, AGARD Conference Proceedings on Radio Systems and Its Ionosphere, Paper 33-1, 1975.
5. Rook, B.J., *Study of the Behaviour and Stability of Phase Fronts on Short Time Scales*, CRC Report 1312, February 1978.
6. Gething, P.J.D., *Radio Direction Finding*, Peter Peregrinus Ltd., England 1978.

